

Safe and Optimal Learning from Preferences via Weighted Temporal Logic with Applications in Robotics and Formula 1

Ruya Karagulle, Cristian-Ioan Vasile, Necmiye Ozay

Abstract—Autonomous systems increasingly rely on human feedback to align their behavior, expressed as pairwise comparisons, rankings, or demonstrations. While existing methods can adapt behaviors, they often fail to guarantee safety in safety-critical domains. We propose a safety-guaranteed, optimal, and efficient approach to solve the learning problem from preferences, rankings, or demonstrations using Weighted Signal Temporal Logic (WSTL). WSTL learning problems, when implemented naively, lead to multi-linear constraints in the weights to be learned. By introducing structural pruning and log-transform procedures, we reduce the problem size and recast the problem as a Mixed-Integer Linear Program while preserving safety guarantees. Experiments on robotic navigation and real-world Formula 1 data demonstrate that the method effectively captures nuanced preferences and models complex task objectives.

I. INTRODUCTION

Autonomous systems are increasingly part of our daily lives, from driverless cars in urban navigation to household robots performing domestic chores. Since these systems operate closely alongside humans, learning from human feedback is a natural way to ensure their behaviors align with human desires. Humans express their preferences in many forms: pairwise comparisons (“I prefer A over B”) [1], rankings (“I prefer A over B, and B over C”) [2], [3], or demonstrations (examples of trajectories or task executions) [4], [5]. Preference learning and learning-to-rank methods leverage comparative judgments to form the queries and collect preference data about behaviors. These preferences are then used in frameworks such as preference-based learning [6], reinforcement learning from human feedback [7], [8], and direct optimization [9], to tune the system behavior. In learning from demonstrations, users directly demonstrate the task or guide the system, often using tools like teleoperation. After the data collection step, these demonstrations are fed into learning frameworks such as behavioral cloning or inverse reinforcement learning.

While these approaches show success in adapting the system behavior based on preferences, they fall short in providing rigorous safety guarantees when the systems are deployed in safety-critical domains, such as autonomous vehicles, medical robotics, and industrial automation. These methods generally assume that users demonstrate and prefer safe options. However, in cases where the user cannot reliably judge safety, this assumption can be dangerous or even fatal for all agents in the environment. The fundamental challenge is to enable learning

within safe behaviors, even in cases where user preferences conflict with safety requirements.

Karagulle et al. offer a solution for the safe preference learning challenge [10], [11]. Combining temporal logic formalism with preference learning using pairwise comparisons, their proposed framework learns the importance order of the sub-tasks and time instances using preference data. More specifically, they express system specifications using Weighted Signal Temporal Logic (WSTL) [12] and learn the weights of the formula. This learned WSTL specification can be used for control synthesis tasks [13]. The framework preserves the qualitative semantics of the task specification, ensuring that the meaning of safety does not depend on learned weights. As WSTL provides a quantitative measure for satisfaction and violation of specifications, the framework guarantees that an unsafe behavior is never favored over a safe one. The authors use gradient-based learning or random sampling for the learning part. While these methods are effective in finding suitable weights, both methods are fundamentally limited in finding the optimal solution in terms of the number of preferences satisfied by the formula. Moreover, gradient-based approaches are susceptible to getting stuck at a local minimum due to the complex nature of the quantitative semantics of the temporal logic. Solving safe preference learning to optimality leads to a Mixed-Integer Problem (MIP) formulation with multi-linear constraints with integers, a hard class of problems to solve.

In this paper, we first extend the safe preference learning problem to richer forms of feedback: pairwise preferences, rankings, and demonstrations. Additionally, we overcome the computational challenges of previous methods by introducing two key procedures. First, *structural pruning* eliminates parts of the formula that do not impact the quantitative semantics for each signal, thus reducing the problem size. We show that structural pruning does not change the quantitative semantics of signals over formulas. Second, *log-transform* linearizes temporal logic constraints, thus enabling the formulation of the problem as a Mixed-Integer Linear Program (MILP). We prove that the log-transformation does not affect the optimizer of the optimization problem. Together, these techniques allow us to achieve efficient and *optimal* learning. This is in contrast to earlier approaches based on heuristic solvers without optimality guarantees [10].

We demonstrate the performance of the proposed method on a safe preference learning problem for a simple robotics navigation task, and a learning-to-rank problem using real-world Formula 1 data. In the robot navigation experiment, we show that the method is sensitive to even small changes in preferences and successfully reflects these differences in the

R. Karagulle and N. Ozay are with the University of Michigan. C. Vasile is with Lehigh University. Corresponding author email: ruyakrgl@umich.edu

This work is supported in part by NSF Grant TI-2303564 and NSF Grant IIS-2442644. The authors thank Gustavo A. Cardona for technical discussions. R. Karagulle thanks Doruk Aksoy, Anil Kayar, Emre Bugdayci, and Can Aksut for Formula 1 discussions.

synthesized trajectories. In the Formula 1 experiment, we illustrate that the learned weights capture complex structures like critical aspects of race performance, effectively modeling race strategies and providing insights into what factors influence successful outcomes over the course of the race.

II. PRELIMINARIES

A. Signal Temporal Logic (STL)

STL is used to reason about signals $\sigma : \mathbb{T} \rightarrow \mathcal{S}$, where $\mathbb{T} \subset \mathbb{Z}_{\geq 0}$ is the time domain and $\mathcal{S} \subseteq \mathbb{R}^m$ is the m -dimensional real-valued signal domain. A well-formed STL formula ϕ follows the grammar $\phi ::= \top \mid \mu \mid \neg \phi \mid \phi_1 \wedge \phi_2 \mid \phi_1 \mathbf{U}_{[a,b]} \phi_2$. Syntax elements have the following interpretations: \top is Boolean truth, μ is a predicate of the form $\mu(\sigma(t)) := h_\mu(\sigma(t)) \geq 0$ where $h_\mu : \mathcal{S} \rightarrow \mathbb{R}$ maps the signal value at time instant t , to a real value². The operator \neg is the negation, \wedge is the conjunction, and $\mathbf{U}_{[a,b]}$ is the ‘‘Until’’ operator³. Subscript $[a, b]$ with $a, b \in \mathbb{Z}_{\geq 0}$ defines the time interval that the temporal operator is acting on. When the time interval includes the whole signal length, we omit the time interval subscript. The qualitative semantics of STL are defined in [14]. If a signal σ satisfies (violates) a formula ϕ at time t , it is shown as $(\sigma, t) \models \phi$ ($(\sigma, t) \not\models \phi$). For qualitative semantics at time instant $t = 0$, we omit t and write $\sigma \models \phi$. STL has quantitative semantics to measure how well the signal satisfies the formula or how badly it violates the formula. There are different quantitative semantics in the literature [14]–[16]. We follow the metric defined in [14], and call it the *robustness*. The robustness of a signal at time t is shown as $\rho(\sigma, \phi, t)$. When $t = 0$, we denote it as $\rho(\sigma, \phi)$. When we work with finite signals, we assume that the signal length covers the time horizon of the formula, a function of time intervals of temporal operators. Additionally, we emphasize that we use STL over discrete-time (as opposed to continuous-time) finite signals with necessary modifications as needed [17].

Each STL formula can be represented by an Abstract Syntax Tree (AST) [18]. In an AST, nodes represent syntactic elements: leaf nodes correspond to predicates or \top , while non-leaf nodes correspond to logical and temporal operators. Edges encode the relationships between operators and their operands in each subformula. Unary operators (Negation, Always, Eventually) have one child node, while binary operators (And, Or, Until) have two. To represent and reason about the robustness more systematically, we represent the robustness computation as a tree. Building on the AST, we define the Robustness Computation Tree (RCT) of a formula ϕ , at time t as $\mathcal{T}_{\phi,t} = (\mathcal{N}_{\phi,t}, \mathcal{E}_{\phi,t})$, where $\mathcal{N}_{\phi,t}$ is the set of nodes, obtained by extending each AST node with the explicit time index at which the corresponding operator or predicate is evaluated during robustness computation, and $\mathcal{E}_{\phi,t}$ is the set of

directed edges encoding parent–child relationships in the time-indexed structure. Placing the signal’s predicate robustness values $h_\mu(\sigma)$ to leaf nodes of $\mathcal{T}_{\phi,t}$, and replacing each operator with its function defined in the quantitative semantics, the tree exactly mirrors the robustness computation for $\rho(\sigma, \phi, t)$, when operations from the leaf nodes to the root node of the tree are followed. Moreover, for any subformula ϕ_i and t' appearing in the formula, the subtree $\mathcal{T}_{\phi_i,t'}$ corresponds to $\rho(\sigma, \phi_i, t')$.

Example 1. Let $\phi = \diamond_{[3,5]}(0 \leq \sigma \leq 5)$ be an STL formula. Figure 1a and 1b show the AST and RCT of ϕ at $t = 0$, respectively. Tree $\mathcal{T}_{0 \leq \sigma \leq 5, t'}$ corresponds to $\rho(\sigma, 0 \leq \sigma \leq 5, t')$.

B. Weighted Signal Temporal Logic (WSTL)

WSTL is tailored to represent priorities and preferences in STL formulas [12]. Its syntax extends STL syntax as $\phi ::= \top \mid \mu \mid \neg \phi \mid \phi_1 \wedge^w \phi_2 \mid \phi_1 \mathbf{U}_{[a,b]}^{w^1, w^2} \phi_2$, where the weights are $w \in \mathbb{R}_{>0}^2$ and $w^1, w^2 : [a, b] \rightarrow \mathbb{R}_{>0}$. All operators are interpreted as in STL. The quantitative semantics of WSTL is called the *weighted robustness*, and defined as [10]:

$$\begin{aligned} r(\sigma, \top, t) &= \infty \\ r(\sigma, \mu, t) &= \rho(\sigma, \mu, t) \\ r(\sigma, \neg \phi, t) &= -r(\sigma, \phi, t), \\ r(\sigma, \phi_1 \wedge^w \phi_2, t) &= \min(w_1 r(\sigma, \phi_1, t), w_2 r(\sigma, \phi_2, t)), \\ r(\sigma, \phi_1 \mathbf{U}_{[a,b]}^{w^1, w^2} \phi_2, t) &= \max_{t' \in [a,b]} \left(\min(w_{t'}^1, \min_{t'' \in [t, t+t']} r(\sigma, \phi_1, t'')) \right. \\ &\quad \left. w_{t'}^2 r(\sigma, \phi_2, t + t') \right). \end{aligned} \quad (1)$$

The derived operators have the following definitions:

$$\begin{aligned} r(\sigma, \phi_1 \vee^w \phi_2, t) &= \max(w_1 r(\sigma, \phi_1, t), w_2 r(\sigma, \phi_2, t)), \\ r(\sigma, \square^w \phi, t) &= \min_{t' \in [a,b]} (w_{t'} r(\sigma, \phi, t + t')), \\ r(\sigma, \diamond^w \phi, t) &= \max_{t' \in [a,b]} (w_{t'} r(\sigma, \phi, t + t')). \end{aligned} \quad (2)$$

To denote the weighted robustness at $t = 0$, we use $r(\sigma, \phi)$. As it is shown in [10], [12], the quantitative semantics in (1) is sound. The RCT can be defined for WSTL formulas as well. Weights of the operators are added as costs to the relevant edges, and we obtain $\mathcal{T}_{\phi, \mathbf{w}, t} = (\mathcal{N}_{\phi, t}, \mathcal{E}_{\phi, t}, \mathbf{w})$.

C. Parametric Weighted Signal Temporal Logic (PWSTL)

To enable learning from data, we treat weights as parameters, and define an extension to WSTL called Parametric Weighted Signal Temporal Logic (PWSTL) (cf. [19]). We denote the set of unknown parameters as \mathcal{W} , and PWSTL formulas as $\phi_{\mathcal{W}}$. The weight set is the set (or a subset) of all possible weights in the formula. A PWSTL formula results in a WSTL formula $\phi_{\mathcal{W}=\mathbf{w}}$ with the valuation \mathbf{w} of the parameters. For simplicity, if it is clear from the context, we write $\phi_{\mathbf{w}}$ to denote the WSTL formula with valuation \mathbf{w} .

III. PROBLEM STATEMENT

Learning from human feedback in autonomous systems broadly encompasses problems such as learning from preferences, demonstrations, or rankings. Classical approaches include inverse reinforcement learning and behavioral cloning,

¹We denote $\rho(\sigma, \phi_i, t')$ as $\rho_{\phi_i}^{\sigma(t')}$ due to space limitations.

²Note that it is possible to transform any (in)equality of the form $f(x) \sim c$, where $\sim \in \{\leq, \geq, =\}$, into the form defined in the syntax.

³Additional operators: disjunction \vee , Always $\square_{[a,b]}$, and Eventually $\diamond_{[a,b]}$ can be derived from the grammar as $\phi_1 \vee \phi_2 = \neg(\neg\phi_1 \wedge \neg\phi_2)$, $\diamond_{[a,b]} \phi = \top \mathbf{U}_{[a,b]} \phi$, and $\square_{[a,b]} \phi = \neg(\diamond_{[a,b]} \neg\phi)$.

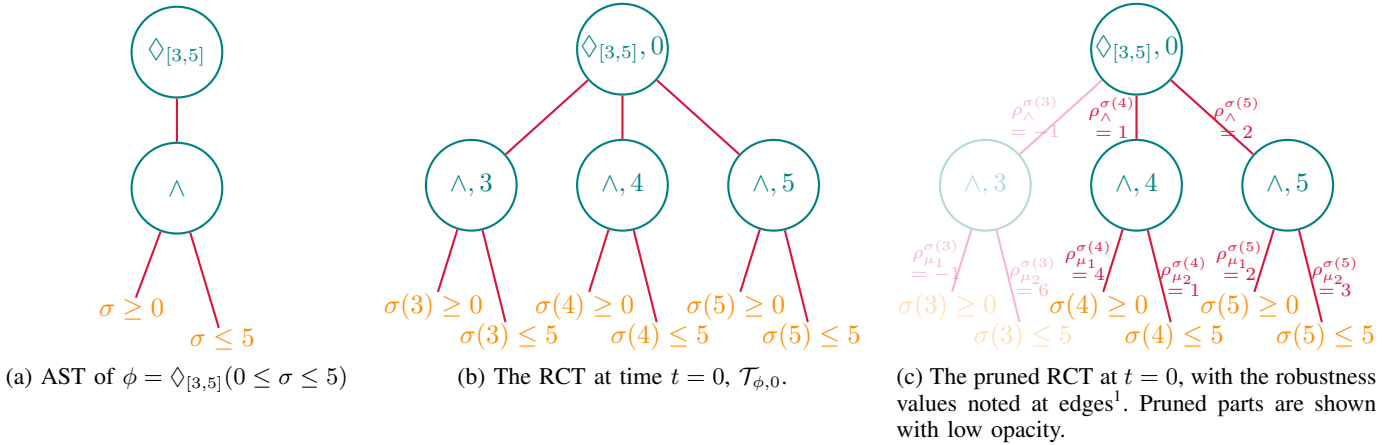


Fig. 1: Trees associated with $\phi = \diamond_{[3,5]}(0 \leq \sigma \leq 5)$; AST, RCT, and pruned RCT for signal $\sigma = [5, 6, 7, -1, 4, 2]$, respectively.

which directly infer policies or reward structures from data [20], [21]. Both methods typically require a reinforcement learning-style framework. In contrast, we propose to learn a utility function that captures the preferences independent of a specific agent or environment. Ideally, this utility function serves as a unifying representation of human intent, and whenever trajectories consistent with these preferences are required, they can be synthesized via downstream trajectory generation methods. To restrict the search space of possible utility functions, we focus on a structured family of functions defined by the safety requirements or task specifications. Particularly, we leverage the expressive power of WSTL to describe specifications and the weighted robustness. By parameterizing weights in the quantitative semantics, we enable different weight valuations to encode potential instantiations of the utility function. The learned WSTL formula can be seamlessly integrated to control synthesis frameworks such as model predictive control (MPC), to generate safe and personalized trajectories. Moreover, as weight valuations represent the importance of subformulas or time instances, the result of the learning framework is interpretable, in contrast to using neural network-like structures for learning.

In other words, learning from human feedback problems via WSTL requires a task description written in STL and a user dataset. It searches for a weighted quantitative semantics that maximizes the problem’s objective. Formally, we define the problem as follows:

Problem 1 (Learning from Human Feedback (LHF)). *Consider an STL formula ϕ and a dataset \mathcal{D} obtained from user feedback. LHF aims to find a weight valuation w^* for ϕ_w , the PWSTL version of the formula ϕ with $|\mathcal{W}| = n$, that maximizes the objective value $f(\phi_w, \mathcal{D})$. That is,*

$$w^* \in \max_{w \in \mathbb{R}_{>0}^n} f(\phi_w, \mathcal{D}) \quad \text{s.t.} \quad \text{dataset constraints} \quad (3)$$

The form of the objective function and dataset constraints depend on the learning setup and the available data. For safe preference learning, the user dataset is given as $\mathcal{PR} =$

$\{(\sigma_{i_1}, \sigma_{i_2}, l_i)\}_{i=1}^P$, where σ_{i_1} and σ_{i_2} are compared and $l_i \in \{1, -1\}$ denotes its label: $l_i = 1$, when σ_{i_1} is preferred over σ_{i_2} and $l_i = -1$ otherwise. The goal is to maximize the number of correctly ordered pairs, leading to the objective function of the form $f(\phi_w, \mathcal{PR}) = \sum_{i=1}^P \mathbb{1}(l_i \Delta_i(w) > 0)$, with constraints $\Delta_i(w) = r(\sigma_{i_1}, \phi_w) - r(\sigma_{i_2}, \phi_w)$. For learning-to-rank, the dataset is an ordered set $\mathcal{R} = \{\sigma_1 \succeq \sigma_2 \succeq \dots \succeq \sigma_P\}$. This can be reformulated as a pairwise preference dataset $\mathcal{PR} = \{(\sigma_i, \sigma_j, 1)\}_{i=1, j=i+1}^{P-1, P}$, reducing the problem to safe preference learning, with the same objective function and $\binom{P}{2}$ constraints. Finally, in learning from demonstrations, we are given a set of “desired” trajectories $\mathcal{D} = \{\sigma_i\}_{i=1}^D$. In this setup, we can use $f(\phi_w, \mathcal{D}) = \sum_{i=1}^D r(\sigma_i, \phi_w)$ as the objective value, which aims to assign high weighted robustness values to desired trajectories.

The computational complexity of WSTL synthesis problems grows with the complexity of the formula. In general, computing the weighted robustness for a signal involves evaluating predicate values at multiple time instances, multiplying them with corresponding weight valuations, and applying nested min/max operations, following the WSTL semantics. Since weights appear multiplicatively, optimizing over them results in a mixed integer program (MIP) with multi-linear constraints, where integers appear as in [22]. As such, weight synthesis problems were solved with heuristic approaches such as gradient descent [23] or sampling [10] in the literature.

IV. REDUCTION TO MILP

In this paper, we propose two procedures to reduce the problem size and linearize the constraints, making the problem easier to solve. The first procedure, called the *structural pruning*, systematically examines how values in the Robustness Computation Tree are propagated to the root node to determine the robustness value of a signal with respect to a formula. Based on this observation, we can prune the branches that cannot affect the robustness value regardless of the weight valuations assigned. The second procedure, called the *log-transform*, leverages the product identity of the logarithm

function to convert constraints in the multiplication form into constraints in the summation form. Since the logarithm is only defined for positive values, a naive approach requires that all subformulas (subtrees in RCT) must have positive robustness for the transformation to be valid, which is a restrictive requirement in practice. To address this, we combine the log-transform with structural pruning, and ensure that only contributing parts with the same robustness value sign of the formula are considered in the robustness computation, therefore making all variables of the constraints that encode this computation have the same sign. Together, these two procedures allow the problem to be reformulated as an MILP with a potentially reduced number of constraints.

Before getting into the details of the procedures, we note that all formulas are assumed to be in positive normal form (PNF), that is, negations appear only in front of predicates. While this assumption is not restrictive, as negations can be pushed to the predicate level, we discuss the rationale later.

A. Structural Pruning

The key insight of the structural pruning is that if the overall robustness of a signal is positive (indicating satisfaction), then any subformula with negative or zero robustness values must be “absorbed” by one of its parent operations in the Robustness Computation Tree. Consequently, when fitting weights to this tree, we know that weights connecting nodes with negative or zero robustness value to their parents cannot change the robustness. This allows us to systematically prune parts of the tree whose values are not actively contributing to robustness.

More formally, consider a signal σ , an STL formula ϕ , and the associated RCT $\mathcal{T}_{\phi,t}$. If $\rho(\sigma, \phi) > 0$, then only the subtrees $\mathcal{T}_{\phi_i,t'}$ with positive robustness values, i.e., $\rho(\sigma, \phi_i, t') > 0$, can potentially determine the final robustness value at the root node of $\mathcal{T}_{\phi,t}$ when weights are introduced to the formula. Similarly, if $\rho(\sigma, \phi) < 0$, then only subtrees with negative robustness values affect the final robustness. Note that if $\rho(\sigma, \phi) = 0$, then there does not exist a weight valuation that can change the weighted robustness values. This observation leads to our structural pruning algorithm, which is recursively defined over the Robustness Computation Tree, and shown in Algorithm 1.

Algorithm 1 Structural Pruning

```

1: function PRUNE( $\sigma, \phi, t, s_\phi$ )
2:   if Root node of  $\mathcal{T}_{\phi,t}$  is an Operator then
3:     for  $(\phi_i, t') \in \text{Children of the Root}$  do
4:       if  $\text{sign}(\rho(\sigma, \phi_i, t')) = s_\phi$  then
5:          $\mathcal{T}_{\phi_i,t} \leftarrow \text{PRUNE}(\sigma, \phi_i, t', s_{\phi_i})$     $\triangleright$  PRUNE child
6:       else
7:          $\mathcal{T}_{\phi,t} \leftarrow \mathcal{T}_{\phi,t} \setminus \mathcal{T}_{\phi_i,t'}$             $\triangleright$  Delete child
8:       end if
9:     end for
10:  else                                      $\triangleright$  Root node of  $\mathcal{T}_{\phi,t}$  is a Predicate
11:    return  $\mathcal{T}_{\phi,t}$                             $\triangleright$  Return the tree
12:  end if
13: end function

```

The algorithm is given a signal, denoted σ , a formula, denoted ϕ , the time instance where the robustness is computed, denoted t , and the sign of the robustness value, denoted $s_\phi = \text{sign}(\rho(\sigma, \phi, t))$. The procedure starts from the root node of the RCT. If this node is an operator, i.e., not a predicate node, then for all children of the operator (line 3), we check the sign of the robustness value of the signal with respect to that child (line 4). If the sign of the child matches with s_ϕ , then we recursively prune the child subtree (line 5); otherwise, we remove this child subtree, since it cannot yield a better value than other children in the min/max operation (line 7). Finally, if we reach a predicate node, as it has the same robustness sign as s_ϕ , we keep that leaf-node (line 11). Note that this algorithm returns at least one node.

Theorem 1. *Given a signal σ and a formula ϕ , structural pruning preserves the quantitative semantics of STL formulas. That is, the robustness value computed from the pruned RCT is $\rho(\sigma, \phi, t)$.*

The proof follows the fact that for any operator, a child whose robustness has an opposite sign from the parent cannot affect the min or max computation. By recursively applying this argument from root to leaves, all removed nodes are non-influential, so the robustness of the pruned formula equals that of the original formula.

Example 1 (continued). Consider ϕ , and $\sigma = [5, 6, 7, -1, 4, 2]$. Figure 1c shows the pruned RCT, $\mathcal{T}_{\phi,t}^{\text{pruned}}$.

Thus far, we have defined structural pruning for STL formulas. Because WSTL semantics are also sound, meaning weights cannot change the sign of the robustness values, the same procedure can be directly applied to WSTL (and PWSTL) formulas, allowing us to prune irrelevant weights as well. Since robustness values with opposing signs do not contribute to the final weighted robustness value, varying their associated weights cannot change the weighted robustness of the signal. Therefore, these weights are not active decision variables. We can then write the robustness constraints based on the pruned RCT of the WSTL formula.

B. The log-transform of constraints

The log-transform is motivated by the desire to linearize the constraints related to the robustness computation in weight synthesis problems. Prior work [22], [24] demonstrated that constraints of the form $\rho(\sigma, \phi) > 0$ can be encoded as a series of mixed-integer linear constraints. In the case of the weighted robustness, however, the temporal and logical operators multiply their operands’ robustness values by the associated weights (see Eq. (1)). Encoding these operations directly, following [12], [22], introduces multi-linearity whenever weights are treated as decision variables.

To address this, we apply a logarithmic transformation to both sides of mixed multi-linear integer constraints and convert the products into sums, thus linearizing them with respect to the weights. While effective in linearizing the product terms, the logarithm is only defined over the positive domain. In its

most naive form, this requires both sides of every constraint to be positive. In other words, this transformation is valid only for signals that satisfy all predicates at all time instances that are used in the robustness computation (therefore, in constraints), which is not realistic. Before introducing our method for extending the transform to arbitrary signals (independent of satisfaction or violation), we first define the log-transform of the robustness functions in Eq. (1) under the assumption that all predicate values are strictly positive. The log-transform of the robustness of signal σ at time t is defined recursively as:

$$\begin{aligned} \log r(\sigma, \top, t) &= \infty, \\ \log r(\sigma, \mu, t) &= \log(h_\mu(\sigma(t))), \\ \log r(\sigma, \phi_1 \wedge^w \phi_2, t) &= \min_{i \in \{1,2\}} (\log(w_i) + \log r(\sigma, \phi_i, t)), \\ \log r(\sigma, \phi_1 \mathbf{U}_{[a,b]}^{w^1, w^2} \phi_2, t) &= \max_{t' \in [a,b]} \left(\min \left(\begin{aligned} &\log(w_{t'}^1) + \log r(\sigma, \phi_2, t + t'), \\ &\log(w_{t'}^2) + \min_{t'' \in [t, t+t']} \log r(\sigma, \phi_1, t'') \end{aligned} \right) \right). \end{aligned} \quad (4)$$

The derived operators are defined as:

$$\begin{aligned} \log r(\sigma, \phi_1 \vee^w \phi_2, t) &= \max_{i \in \{1,2\}} (\log(w_i) + \log r(\sigma, \phi_i, t)), \\ \log r(\sigma, \diamond_{[a,b]}^w \phi, t) &= \max_{t' \in [a,b]} (\log(w_{t'}) + \log r(\sigma, \phi, t + t')), \\ \log r(\sigma, \square_{[a,b]}^w \phi, t) &= \min_{t' \in [a,b]} (\log(w_{t'}) + \log r(\sigma, \phi, t + t')). \end{aligned} \quad (5)$$

We can still convert the right-hand sides of Eqs. (4) and (5) into a series of mixed-integer linear constraints using [22]. Note that we do not define the log-transform for the robustness computation of negation. The restriction arises due to the domain in which the logarithm is defined: for a formula ϕ , if $\log(r(\sigma, \phi))$ is defined, then $\log(r(\sigma, -\phi))$ is not, and vice versa. In consequence, negation is not allowed in the formulas, which restricts our attention to formulas in PNF only. Negation in front of predicates is not an issue since it can be carried inside predicates by reverting the inequality.

When applying the log-transform to constraints in Problem 1, $\log(h_\mu(\sigma(t)))$ are computed apriori. The decision variables are $\log(w_i)$. We perform a change of variables $v_i = \log(w_i)$ during optimization, leaving the constraints log-free. We can recover the original weights via $w_i = \exp(v_i)$ afterward. Similarly, the robustness of the weighted formula can be recovered as $r(\sigma, \phi, t) = \exp(\log r(\sigma, \phi, t))$ directly from the transformed constraints, without recomputing it from scratch. Next, we show that applying log-transformation preserves the maximizer of Problem 1.

Theorem 2. *Consider Problem 1 with an STL formula ϕ and a dataset \mathcal{D} . Assume \mathcal{D} consists of signals that satisfy all predicates of ϕ at all time instances that are required to compute $\rho(\sigma, \phi)$. Then, applying the log-transform to the robustness constraints does not change the optimizer of Problem 1.*

Proof. The logarithm is a strictly increasing function, and therefore preserves the ordering of all min and max operations in the formula. That is, for any set of $a_1, \dots, a_n \in \mathbb{R}_{>0}$, we have $\log(\min(a_1, \dots, a_n)) = \min(\log(a_1), \dots, \log(a_n))$, and

similarly for max. Hence, while the numerical values of each operation in the Robustness Computation Tree change, the optimizers remain unchanged. \square

We now discuss how to relax the positivity assumption, i.e., handling signals whose robustness computation constraints contain non-positive values. Two cases need to be considered: signals with all negative values, and signals with mixed values.

For signals whose robustness computation contains only negative robustness values, e.g., signals which violate all predicates of a formula at all time instances needed for the robustness computation, we cannot use log-transform directly. However, because all these values lie in the negative quadrant, we can still compare them using the logarithm of their absolute values. Therefore, we can separate the sign from the magnitude, take the logarithm of the absolute value and multiply it with negative before performing the min/max operations, obtaining equations such as $\min_{i \in [1,2]} (-(\log(w_i) + \log(|r(\sigma, \phi_i, t)|)))$. Equivalently, this can be handled by reversing the operator: for example, taking max instead of min when the values are negative, and removing the negative sign.

For signals whose robustness computation contains a mix of positive and negative values, we leverage the structural pruning algorithm to unify the signs in the computation. Applying structural pruning to a signal's robustness computation allows us to remove any subtree that results in a robustness value whose sign is different than the sign of the robustness value at the root node. Pruning ensures that all remaining constraints have robustness values with the same sign, allowing the log-transform to be applied safely to either all-positive robustness values or all-negative robustness values. Similar to the only-positive case, we show that applying these two procedures sequentially in a learning from human feedback problem does not change the maximizer of the problem.

Theorem 3. *Consider Problem 1 with an STL formula ϕ and a dataset \mathcal{D} . Applying structural pruning to the signals in \mathcal{D} and the log-transform to the robustness constraints does not change the optimizer of the problem.*

Proof. The proof directly follows Theorems 1 and 2. Structural pruning removes only subtrees that cannot influence the overall robustness of each signal. The log-transform preserves the ordering of all min and max operations for the remaining positive or negative values. Therefore, the combination of pruning and logarithmic transformation does not change the optimizer of the original problem. \square

With the structural pruning and log-transform procedures, we substantially reduce the problem size and convert the inherently multi-linear constraints into a linear form, yielding a computationally efficient method for optimally solving learning from human feedback problems. Specifically, the maximizer of Problem 1 w^* , produces a WSTL formula ϕ_{w^*} whose qualitative semantics ensure that safety constraints are never violated—regardless of the learned weights. Furthermore, each learned weight in w^* provides direct interpretability, as its value quantifies the relative importance of the corresponding

subformula or time instance in determining the overall robustness. Thus, our approach not only guarantees safety but also facilitates transparent personalization by highlighting which task components most strongly reflect the user’s preference.

V. EXPERIMENTS

To evaluate the performance of the proposed method, we focus on two experiments: safe preference learning for robot navigation tasks, and interpretable learning-to-rank using real-life Formula 1 data.

A. Safe Preference Learning for Robot Navigation

In this experiment, we consider a simple robot navigation task. The robot starts at $(x, y) = (1, 1)$, must visit either region $A = [7, 9] \times [1, 3]$, or region $B = [1, 3] \times [7, 9]$, within the first 10 seconds. It should then proceed to region $C = [7, 9] \times [7, 9]$ within the next 10 seconds while always staying in the environment bounds $E = [0, 10] \times [0, 10]$, and avoiding the unsafe region $U = [3, 6] \times [3, 6]$. This task is represented by the STL formula $\phi = \diamond_{[0,10]}((x, y) \in A \vee (x, y) \in B) \wedge \diamond_{[10,20]}\square((x, y) \in C) \wedge \square_{[0,20]}\neg((x, y) \in U) \wedge \square_{[0,20]}((x, y) \in E)$. The robot follows a double-integrator model:

$$q[t + 1] = \begin{bmatrix} 1 & 1 & 0 & 0 \\ 0 & 1 & 0 & 0 \\ 0 & 0 & 1 & 1 \\ 0 & 0 & 0 & 1 \end{bmatrix} q + \begin{bmatrix} 0 \\ 1 \\ 0 \\ 1 \end{bmatrix} u, \quad u = \begin{bmatrix} a_x \\ a_y \end{bmatrix}, \quad (6)$$

where the state $q[t] = [x \ v_x \ y \ v_y]^T$ represents robot’s current position and velocity. We begin by randomly sampling weight valuations ten times to generate a trajectory for each of the WSTL formulas using PyTelo [25], and form five trajectory pairs. From these, we construct three preference datasets: PD1, the original set of preferences; PD2, obtained by flipping the preference of a single pair in PD1; PD3, obtained by inverting all preferences in PD1. For each preference dataset, we solve the MILP problem to learn the weight valuations that best represent the given preferences, yielding formulas $\phi_w^{\text{PD}i}$. Finally, we synthesize trajectories that will maximize the weighted robustness of the corresponding $\phi_w^{\text{PD}i}$. Figure 2 shows the synthesized trajectories. The results demonstrate that our method is sensitive to even small preference changes and reflects this diversity by producing distinct task executions.

B. Learning-to-rank

For the learning-to-rank example, we consider a real-world motorsport setting: Formula 1. Formula 1 is a wheel-to-wheel race where the goal is to finish in the highest position after a fixed number of laps. Drivers are ranked based on their finishing times, and each team, consisting of two drivers racing, heavily relies on on-track data to determine their race strategies, such as pit stops, tire compound selection, overtake plans, etc. Our goal is to learn a WSTL formula that captures the important aspects of racing on a specified track using previous years’ race data and ranking results. The learned WSTL formula represents an ideal race performance.

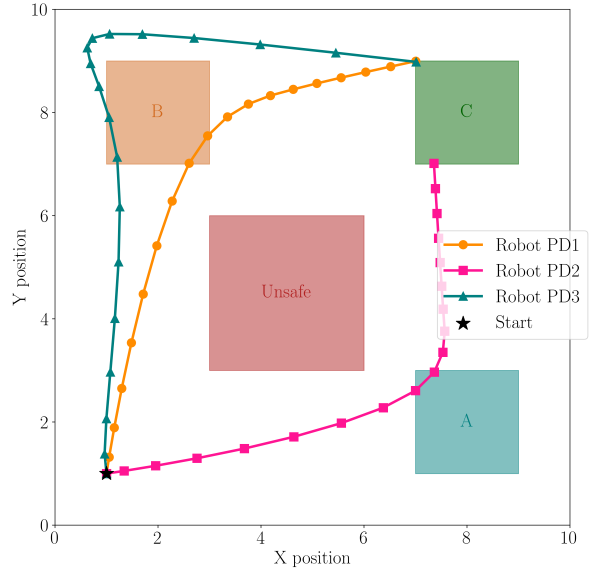


Fig. 2: Trajectories generated using three different preference sets. PD1 is the original preference set, PD2 is obtained by flipping the answer to a single pair in PD1, and PD3 is obtained by reverting all answers in PD1.

A good race performance can be characterized by: starting from a competitive grid position, finishing the race, recording consistently fast lap times, outperforming (and overtaking) the car ahead, executing as few as necessary efficient pit stops, and avoiding on-track issues that affect the lap time, such as collisions and penalties [26]. To encode these principles in STL formalism, we consider several per-lap signals obtained via FastF1, a Python library for analyzing Formula 1 data [27]. Let N be the number of laps run in a race. The percentage of laps completed by a car is $r_{lap} \in [0, 1]^N$. If a car retires early or is lapped, $r_{lap} < 1$. The time-in-pit $t_{pit} \in \mathbb{R}^N$ records the duration of a pit stop on each lap, and is computed from the car’s entry and exit times in the pit lane (zero if no pit stop occurs). The fuel-and-pit-corrected lap times $\bar{t}_{lap} \in \mathbb{R}^N$ adjust the raw lap times for both pit-stop duration and the reduction in car mass due to fuel consumption, and computed for each lap $k \in \{1, \dots, N\}$ as $\bar{t}_{lap}(k) = t_{raw}(k) - (m_{full} - c_{kg/lap}k)s_{s/kg} - t_{pit}(k)$ where $m_{full} = 100$ represents the mass of the fully fueled car, $c_{kg/lap}$ represents the fuel use per each lap, and $s_{s/kg} = 0.033$ represents mass sensitivity of lap time [28]. The position p records the current race ranking of the car. The delta-to-lead $t_{\Delta lead}$ records the lap time differences between the ego and the car in front. Finally, the safety car presence $b_{SC} \in \{-1, 1\}^N$ is set to 1 during the Safety Car and Yellow Flag periods (i.e., when cars reduce speed) and -1 otherwise.

Using these signals, we define the formula characterizing the performance as $\phi = \phi_{complete} \wedge \phi_{grid} \wedge \phi_{\Delta lead} \wedge \phi_{lap} \wedge \phi_{pit}$, where $\phi_{complete} = \diamond(r_{lap} \geq 0)$ represents the effect of finishing the race, $\phi_{grid} = \square_{[0,1]}(p \leq 20)$ represents the

effect of the starting position, $\phi_{\Delta lead} = \square(t_{\Delta lead} \leq 20s)$ represents the effect of competitiveness, $\phi_{lap} = \square(-b_{SC} \implies \bar{t}_{lap} \leq 150s)$ represents the effect of the lap times excluding the reduce-speed periods, and $\phi_{pit} = \diamond(t_{pit} > 0 \implies t_{pit} \leq 30s)$ represents the effect of having efficient pit stops.

To evaluate the accuracy of the ranking learner, we use the normalized Kendall- τ distance, which measures the percentage of discordant pairs, i.e., incorrectly-ordered pairs, in all pairwise comparisons (i, j) where $i \in \{1, \dots, P-1\}$ and $j \in \{i+1, \dots, P\}$. That is,

$$\text{acc}((\sigma_1, \dots, \sigma_P)) = \frac{\text{number of discordant pairs}}{\binom{P}{2}}.$$

Experiment details: To ensure consistent racing conditions over the years, such as weather and safety car appearances, we focus on the Monza Grand Prix. Since there are no major regulation changes in recent years, we use data from 2021, 2022, and 2024 for training, and the 2025 race for testing. The 2023 Monza Grand Prix is excluded due to a false start that shortened the race to 51 laps instead of the usual 53. For both training and test data, we scale all signals at each year to $[0, 1]$ by min-max normalization, to avoid biases due to the order-of-magnitude difference across channels. Because real races involve unpredictable events such as collisions and technical failures, we perform two sets of experiments: one excluding Did Not Finish (DNF) and Did Not Start (DNS) cars and one including them.

For both cases, we warm start the MILP solver by selecting the best-accuracy solution among $S = 10000$ uniform random weight samples (cf. Random Sampling (RS) method of [10]). We then solve the MILP problem with a four-hour time limit, and report the best solution found. As a baseline comparison, we repeat the RS method 1000 times with $S_{RS} = 1000$ weight samples, and report the mean and standard deviations of accuracies. Table I shows the results on training and test sets. It is important to note that even though a global optimal is not guaranteed when the solver is time-limited, the MILP procedure improves over mean RS performance, which shows almost 10% variability on the test accuracy. Also, when compared to its warm-started accuracy, our method raises the accuracy by up to 5%. Moreover, the learned weights generalize to future seasons with different cars, different teams, and different drivers. This highlights the fact that, although driver skills and car performances are at the core of the race success, the proposed method can capture driver-and car-agnostic performance points.

When we take a closer look at the learned weights, we see that, for the DNF/DNS excluded case, the most important part of the formula is the initial grid position, followed by lap times, pit times, delta-to-lead, and completion. On the other hand, when DNF/DNS is included, the importance order changes to first the lap times, followed by the completion, initial grid position and pit times, and finally, delta-to-lead. These insights can help teams improve their race-day strategies.

Finally, we want to answer the following question: given only the laps observed so far until lap K , how accurately can

TABLE I: Performance statistics of RS, and the performance of the proposed method on training and test sets.

Accuracy (%)	DNF/DNS excluded		DNF/DNS included	
	Train	Test	Train	Test
RS [10]	83.8% \pm 0.6%	84.8% \pm 1.3%	78.5% \pm 0.7%	76.6% \pm 9.7%
Ours	86.87%	84.97%	84.21%	81.05%

we predict the final standings? Figure 3 shows the evolution of the prediction accuracy over the race. More specifically, when DNF/DNS are excluded, as Figure 3a shows, the model reaches over 85% accuracy after the first five laps. This observation may indicate that when unpredictable events are not considered, the performance patterns emerge early. On the other hand, when DNF/DNS are included, the accuracy improves more slowly over laps, reflecting the unpredictable nature of the race events.

It is worth emphasizing that the goal of this experiment is not to provide insights on Formula 1 but to serve as a proof-of-concept. The results highlight the abilities of temporal logic learning in analyzing and learning patterns in an interpretable and efficient manner for complex problems like learning-to-rank on real-world sequential data, such as racing.

VI. CONCLUSION, LIMITATIONS AND FUTURE WORK

In this work, we proposed a safe learning-from-human-feedback framework using temporal logic formalism that can be efficiently solved to optimality. The framework consists of two key procedures, structural pruning and log-transform. Structural pruning systematically removes parts of the robustness tree that do not affect the robustness value, reducing the problem size. The log-transform linearizes the robustness computation constraints with respect to weights, enabling an MILP formulation. We demonstrated the performance of the proposed method on two experiments: the preference learning problem for a robot navigation task and the learning-to-rank problem using Formula 1 data. Results show that the method can capture and reflect diverse preferences effectively.

Despite the success of the proposed method in the experiments, several factors may limit its applicability. First, the method requires domain knowledge and expertise in writing temporal logic formulas to define task specifications. While this need introduces a reliance on expert input, it comes with the benefit of interpretability. Second, MILP formulation requires linear objective functions, which may restrict the applicability to problems that involve non-linear objectives or require certain forms of regularization. Looking forward, we plan to integrate more streamlined task specification methods, potentially using large language models to translate plain sentences to STL formulas.

REFERENCES

- [1] D. Shin, A. Dragan, and D. S. Brown, "Benchmarks and algorithms for offline preference-based reward learning," *Trans. on Machine Learning Research*, 2023.
- [2] V. Myers, E. Biyik, N. Anari, and D. Sadigh, "Learning multimodal rewards from rankings," in *Proc. of the 5th Conf. on Robot Learning*, vol. 164, 2022, pp. 342–352.

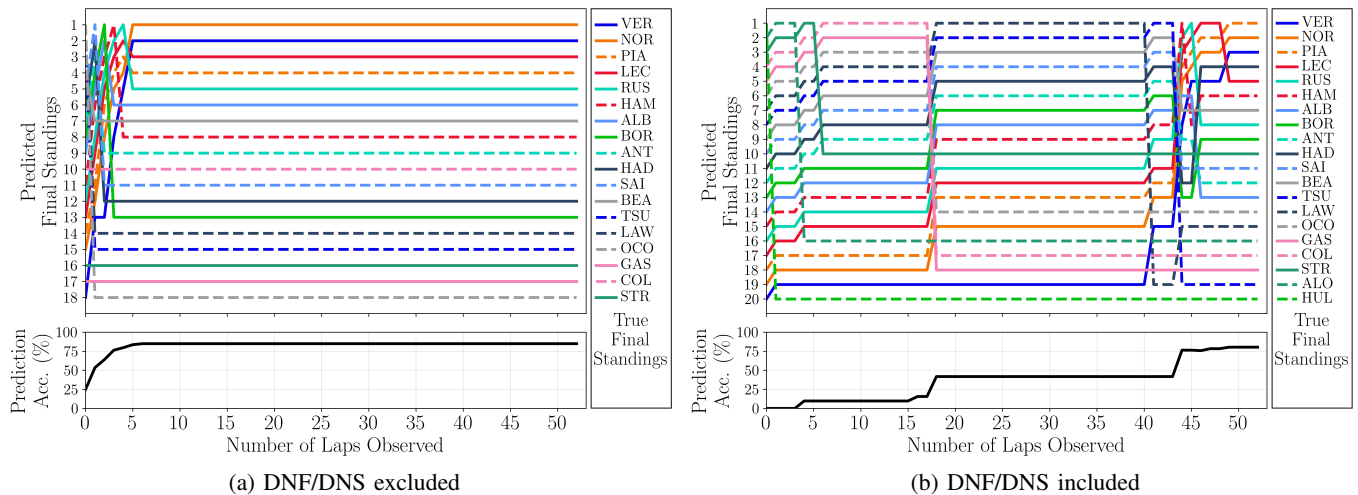


Fig. 3: The evolution of final standing predictions and the prediction accuracy over the laps at the 2025 Monza Grand Prix. The right block shows the correct standing when DNFs are included and excluded. Each team is represented with a separate color, and drivers from the same team are represented with solid and dashed lines. For readability purposes, driver abbreviations are kept instead of enumerations.

[3] D. S. Brown, W. Goo, and S. Niekum, “Better-than-demonstrator imitation learning via automatically-ranked demonstrations,” in *Proc. of the Conf. on Robot Learning*, vol. 100, 2020, pp. 330–359.

[4] M. L. Schrum, E. Sumner, M. C. Gombolay, and A. Best, “Maveric: A data-driven approach to personalized autonomous driving,” *IEEE Trans. on Robotics*, vol. 40, pp. 1952–1965, 2024.

[5] J. de Heuvel, N. Corral, L. Bruckschen, and M. Bennewitz, “Learning personalized human-aware robot navigation using virtual reality demonstrations from a user study,” in *2022 31st IEEE Intl. Conf. on Robot and Human Interactive Communication*, 2022, pp. 898–905.

[6] E. Blyk, “Learning preferences for interactive autonomy,” Ph.D. dissertation, Stanford University, 2022.

[7] P. F. Christiano, J. Leike, T. B. Brown, M. Martic, S. Legg, and D. Amodei, “Deep reinforcement learning from human preferences,” in *Proc. of the 31st Intl. Conf. on Neural Information Processing Systems*, 2017, p. 4302–4310.

[8] D. J. H. III and D. Sadigh, “Few-shot preference learning for human-in-the-loop rl,” in *Proc. of The 6th Conf. on Robot Learning*, vol. 205, 2023, pp. 2014–2025.

[9] G. An, J. Lee, X. Zuo, N. Kosaka, K.-M. Kim, and H. O. Song, “Direct preference-based policy optimization without reward modeling,” in *Advances in Neural Information Processing Systems*, vol. 36, 2023, pp. 70 247–70 266.

[10] R. Karagulle, N. Aréchiga, A. Best, J. DeCastro, and N. Ozay, “A safe preference learning approach for personalization with applications to autonomous vehicles,” *IEEE Robotics and Automation Letters*, vol. 9, no. 5, pp. 4226–4233, 2024.

[11] R. Karagulle, N. Ozay, N. Arechiga, J. Decastro, and A. Best, “Incorporating logic in online preference learning for safe personalization of autonomous vehicles,” in *Proc. of the 27th ACM Intl. Conf. on Hybrid Systems: Computation and Control*, 2024, pp. 1–11.

[12] N. Mehdipour, C.-I. Vasile, and C. Belta, “Specifying user preferences using weighted signal temporal logic,” *IEEE Control Systems Letters*, vol. 5, no. 6, pp. 2006–2011, 2021.

[13] R. Karagulle, M. A. Valdez Calderon, and N. Ozay, “4c: Custom-and-correct-by-construction controller synthesis using multi-modal human feedback,” *IFAC-PapersOnLine*, vol. 58, no. 30, pp. 254–259, 2024, 5th IFAC Workshop on Cyber-Physical Human Systems.

[14] A. Donzé and O. Maler, “Robust satisfaction of temporal logic over real-valued signals,” in *Formal Modeling and Analysis of Timed Systems*. Springer Berlin Heidelberg, 2010, pp. 92–106.

[15] P. Varnai and D. V. Dimarogonas, “On robustness metrics for learning stl tasks,” in *2020 American Control Conf. (ACC)*, 2020, pp. 5394–5399.

[16] N. Mehdipour, C.-I. Vasile, and C. Belta, “Generalized Mean Robustness for Signal Temporal Logic,” *IEEE Trans. on Automatic Control*, vol. 70, no. 3, pp. 1949–1956, 2025.

[17] G. De Giacomo and M. Y. Vardi, “Linear temporal logic and linear dynamic logic on finite traces,” in *Proc. of the Twenty-Third Intl. Joint Conf. on AI*, 2013, pp. 854–860.

[18] X. Li, G. Rosman, I. Gilitschenski, C.-I. Vasile, J. A. DeCastro, S. Karaman, and D. Rus, “Vehicle trajectory prediction using generative adversarial network with temporal logic syntax tree features,” *IEEE Robotics and Automation Letters*, vol. 6, pp. 3459–3466, 2021.

[19] R. Yan, A. Julius, M. Chang, A. Fokoue, T. Ma, and R. Uceda-Sosa, “Stone: Signal temporal logic neural network for time series classification,” in *2021 Intl. Conf. on Data Mining Workshops (ICDMW)*, 2021, pp. 778–787.

[20] E. Blyk, D. P. Losey, M. Palan, N. C. Landolfi, G. Shevchuk, and D. Sadigh, “Learning reward functions from diverse sources of human feedback: Optimally integrating demonstrations and preferences,” *Intl. J. Robotics Research*, vol. 41, no. 1, p. 45–67, Jan. 2022.

[21] S. Griffith, K. Subramanian, J. Scholz, C. L. Isbell, and A. L. Thomaz, “Policy shaping: Integrating human feedback with reinforcement learning,” in *Advances in Neural Information Processing Systems*, vol. 26. Curran Associates, Inc., 2013.

[22] G. A. Cardona, D. Kamale, and C. I. Vasile, “STL and wSTL control synthesis: A disjunction-centric mixed-integer linear programming approach,” *Nonlinear Analysis: Hybrid Systems*, vol. 56, p. 101576, 2025.

[23] K. Leung, N. Aréchiga, and M. Pavone, “Backpropagation through signal temporal logic specifications: Infusing logical structure into gradient-based methods,” *The Intl. J. of Robotics Research*, vol. 42, no. 6, pp. 356–370, 2023.

[24] V. Raman, A. Donzé, M. Maasoumy, R. M. Murray, A. Sangiovanni-Vincentelli, and S. A. Seshia, “Model predictive control with signal temporal logic specifications,” in *53rd IEEE Conf. on Decision and Control*, 2014, pp. 81–87.

[25] G. A. Cardona, K. Leahy, M. Mann, and C.-I. Vasile, “A flexible and efficient temporal logic tool for python: Pytelo,” *arXiv preprint arXiv:2310.08714*, 2023.

[26] C. L. W. Choo, “Real-time decision making in motorsports: analytics for improving professional car race strategy,” Master’s thesis, Massachusetts Institute of Technology, 2015.

[27] P. Schaefer, <https://pypi.org/project/fastf1/>, 2025, version 3.6.1.

[28] A. Heilmeier, M. Graf, and M. Lienkamp, “A race simulation for strategy decisions in circuit motorsports,” in *2018 21st Intl. Conf. on Intelligent Transportation Systems*, 2018, pp. 2986–2993.